Pioneer. Adv. Mater. 2026, 2(1): 1-13 DOI: 10.48308/piadm.2026.245998.1031

Shahid Beheshti University

Pioneering Advances in Materials

Journal homepage: http://piadm.sbu.ac.ir ISSN: 3115-7114

Research paper

Investigation of the Effect of Different Sizes and Shapes on the Photo-thermal and Nonlinear Responses of Nano-Silver

Nada A. Mohammed, Hassan A. Majeed, Ahmed K. Kodeary*

Department of Laser Physics, College of Science for Women, University of Babylon, Hilla, Iraq

*ahmed.kodeary88@uobabylon.edu.iq

Article info:

Article history:

Received: 17/08/2026

Accepted: 04/09/2026

Keywords:

Silver nanoparticles, Silver nanowire, Silver nano-hexagonal, Photo-thermal response, Thermo-plasmonic, Nonlinear response, Z-scan technique

Abstract

The present experimental study focuses on improving the photo-thermal and nonlinear responses of nano-silver across different sizes and shapes. Samples include; spherical silver nanoparticles (Ag NPs) of various sizes (20, 50, and 68 nm), prepared via the Laser Ablation in Liquid (LAL) method using a Nd:YAG pulsed laser at different energies (100, 300, and 500 mJ) respectively. Additionally, silver nanowires (Ag NWs) with different wire diameters (50, 100, and 200 nm) were obtained from the German company Plasma Chem. Furthermore, silver nano-hexagonal structures (Ag NHs) were also examined with different sizes (50, 100, and 200 nm), which were synthesized by the chemical reduction method. The dispersion of all samples was carried out in deionized distilled water (DW) with a refractive index of 1.33, and analyzed using UV–Vis spectroscopy, TEM, FE-SEM, and photothermal response measurements by monitoring the nano-silver samples 405 nm CW lasers at 50 mW for 4 minutes, the local temperature elevation of the samples was recorded. In addition, the Z-scan technique was employed to evaluate the nonlinear refractive index and nonlinear optical responses of all investigated samples. The results showed that the plasmonic properties as well as the linear and nonlinear optical properties can not only be tuned by controlling the shape and size of the nano-silver but also leading to a marked enhancement in thermo-plasmonic behavior with respect to temperature elevation. Additionally, experimental findings demonstrated that the laser-induced temperature elveation of nano-silver holds great promise for sterilizing and disinfecting medical devices.

1. Introduction

Nanotechnology has recently witnessed a qualitative leap, particularly in the fields of nonlinear optics and thermo-optical physics [1-5]. Nano-Silver stands out as one of the most scientifically interesting materials, due to their unique localized surface plasmon resonance (LSPR) properties, which make them ideal candidates for applications ranging from medical diagnostics to optical data processing technologies [6, 7].

The primary objective of this study is to explore the relationship between the structural geometry of these particles in their various forms such as spherical, nanowire, and hexagonal shapes and their response to photo-catalytic stimulation [8]. Understanding how "size" and "shape" influence the nonlinear refractive index and thermal response has long been a major challenge for researchers in this field; precise control of these parameters is key to enhancing plasmonic properties and adapting them for specific technological applications [9-13].

This research adopted an integrated experimental approach based on comparing the response of geometrically diverse samples under controlled energy conditions.

By using advanced techniques such as Z-scan and spectroscopic measurements, we aim to provide a clear view of how these thermal changes resulting from the photochemical reaction can be exploited in practical applications, most notably in bio-sterilization processes and advanced medical fields.

This opens new horizons for developing devices that rely on the superior optical and thermal properties of silver nanoparticles.

There are several shapes and sizes of nano-silver as shown in Figure 1 [14, 15], but in this study we highlight spherical nano-silver and compare the results with silver nanowires and silver nano-hexagonal structures.

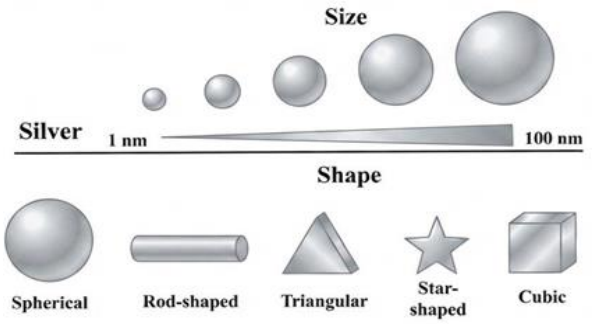

Figure 1. Illustration of a nano-silver with different sizes and shapes

2. Experimental Work

The current work includes synthesis methods and characterization techniques for the nano-silver used in this study, comprising a total of nine samples of nano-silver with different sizes and shapes. Three samples of spherical silver nanoparticles (Ag NPs) with different size (20, 50, and 68nm), and three samples of silver nano-hexagonal (Ag NHs) with different size (the diameter of 50, 100, and 200 nm), as well as three samples of silver nanowires (Ag NWs) with different diameter (50, 100, and 200 nm), with lengths less than 50 microns.

To synthesize nano-silver using laser ablation in aqueous solutions (LAL) method, to fabricate the spherical silver nanoparticles, and used chemical reduction method to fabricate the silver nano-hexagonal, while the silver nanowires were purchased from the German PlasmaChem company. A Nd:YAG pulsed laser with variable pulse energy (100, 300, and 500 mJ) is used in the LAL experiment to generate the Ag NPs, this laser operates at wavelength 1064 nm, 6 Hz repetition rate, and 5 ns pulse width. The pulsed laser focused directly by lens (convex lens with 150mm focal length) on silver target (purity 99.9% with 2 mm target thickness). The silver target is placed inside a container immersed in deionized water (DW), during irradiation with pulse laser for 4 minutes, as in Figure 2-a. The aqueous solution is maintained at 10 mm over the target to obtain a

suitable concentration of the silver nanoparticles, with changing the laser pulse energy (100, 300, and 500 mJ) to obtain different sizes of the Ag NPs, as a result different size (20, 50, and 68 nm) respectively. Ions (Ag+) by hydroxylamine. The chemical reduction in liquid is a common method for synthesizing the Ag NHs, because it is easy to prepare and has a low cost, as well as facilitates control of the size and shape of the nanomaterial, provides high purity index, and thermal stability. The colloidal suspensions of the Ag NHs were prepared by reduction of Ag+ using Hydroxylamine and Trisodium citrate as reducing agents, which were added in different steps of the experiment to complete the reduction. The method used to prepare the Ag NHs can be summarized as follows:

In the first step, mixing 500µl of Hydroxylamine (0.06M) and 500µl of NaOH (0.05M) to formulate the initial solution. In the second step, while agitating the solution on a vibration plate, 9 ml of $AgNO_3$ (10^{-3} M) was slowly added dropwise, at room temperature. After the mixture turned brown and was left for 5 min, then 100µl of Trisodium citrate (4.13×10^{-2} M) was added to it.

The final mixture has been shaken for 15 min, then the mixture changes to dark gray color, the reduction with Hydroxylamine leads to the formation of the Ag NHs. Total Reaction Volume = 500 µl (Hydroxylamine) + 500 µl (NaOH) + 9 ml (AgNO3) + 100 µl (Trisodium citrate) = 10.1 ml. The pH of the reaction is in the range of (10.5 to about 11.5), since the reaction takes place in a forced alkaline environment created by NaOH to activate the reduction of silver. To determine the total reaction time, slowly add $AgNO_3$ (drop by drop with shaking). Allow the mixture to stand for 5 minutes after it turns brown. Shake the final mixture after adding trisodium citrate for 15 minutes (the total reaction time can be considered related to this). Agitation/Stirring Rate; the mixture is stirred on a vibration plate and shaken for 15 minutes. The speed or stirring rate is very slow. The final concentrations can be calculated after mixing the additives in the total volume to obtain an approximate final concentration of 8.91×10^{-4} M for each reaction. Three sizes of the Ag NHs (50, 100, and 200 nm) were prepared which can be set by controlling the amount of $AgNO_3$, hydroxylamine, and Trisodium citrate. The images of the aqueous suspensions of the nine samples can be seen in Figure 2-d, the distinctive colors of the aqueous suspensions, due to the presence of the SPR absorption spectrum of the nano-silver that changes thusly as per their sizes, shapes and diameters of the nano-silver [16]. It is known that nano-silver is the plasmonic metal that has the property of converting light into heat within the absorption spectrum range; this is called the photo-thermal response [17].

Accordingly, the absorption of the nano-silver is exploited in determining temperature rise by applying a suitable illumination compatible with the wavelength of the thermo-plasmonic property. For this purpose, a high-resolution thermal camera (model of FLIR) is used to record thermo-plasmonic images of samples.

During plasmonic imaging, the samples are irradiated by 405 nm continuous laser with 50 mW power for 5 minutes to record the temperature elevation, which is caused by the conversion of light-to-heat with help of the plasmonic nano-silver, the experimental setup is as shown in Figure 2-b.

The IR camera can convert the infrared energy emitted from the objects to an electronic images, it shows the temperature of the object surface as a thermal image.

The IR camera has optical elements focus IR energy on detector chip which contains many detector pixels (arranged as grid), each pixel converts the incident IR energy on it to signal, then these signals goes to the camera processor which creates a color map sends to the camera memory then the camera displays a color image represent the temperature of the surface object.

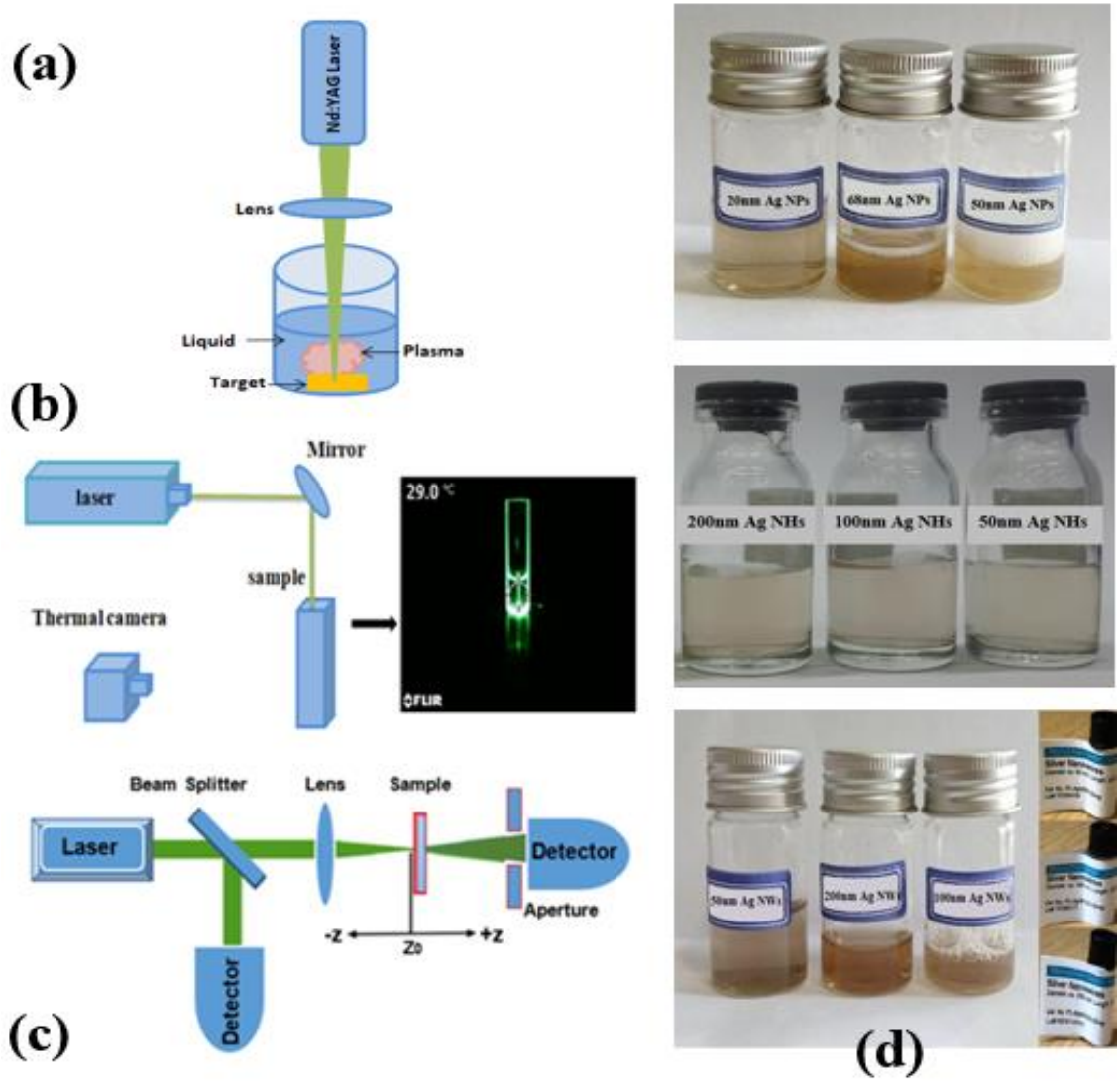

Figure 2. (a) the experimental setup of the laser ablation in aqueous solutions method, (b) the experimental setup of the thermo-plasmonic imaging, (c) the experimental setup of the closed aperture z-scan technique, and (d) the images of the aqueous suspensions of all samples, and images of the Ag NWs packaging as received from the supplier company

In general, a key issue examined here is the convertibility of light into the heat of the plasmonic nano-silver with different sizes and shapes. Finally, to measure the nonlinear refractive index of all samples, the closed aperture z-scan technique is used. For this purpose, a continuous laser operates a power of 50 mW at wavelength 405nm, since this wavelength is suitable for the LSPR spectrum to excite the nano-silver. The laser beam is focused onto the sample using a convex lens with a bore of 15 cm. The experimental setup of the z-scan technique is shown in Figure 2-c. The parameters of the z-scan setup (laser beam waist (w_0) of 0.025 mm, Rayleigh length (z_0) of 4.85 mm, sample thickness of 1 mm (quartz cuvette), aperture size & transmittance (S) of 0.1, detector type of high-efficiency silicon detector, scanning range & speed from −z to +z over a range of 40 cm at a speed of 25 micrometers per second. In order to characterize the specifications of the nano-silver used in this work, we use several techniques

including the UV-visible spectrometer, the FE-SEM microscope, the TEM microscope, the thermal imaging, and the Z-scan method, which are used to determine each of optical absorption, shape and size of particle, photo-thermal response, and nonlinear refractive index; respectively.

3. Result and dissection

The position and intensity results of the LSPR of the nano-silver are determined from the optical absorption spectra; they are shown in Figure 3. The absorbance peak of the Ag NPs with different sizes displayed in Figure 3-a, one can observe that the peak intensity increases with increasing the Ag NPs size with a red shift in the LSPR position from 401nm to 411nm. This increase in intensity and position is due to the increase in the refractive index and concentration of the aqueous suspensions due to the increase in the size of the nanoparticles, where it is known that the properties of the SPR depend on the size of the plasmonic nanoparticles, this result agrees with Ref [17].

In addition, the absorption spectra of the Ag NWs dissolved in deionized water with different diameters (50, 100, and 200 nm) are shown in Figure 3-b. It can be seen that the absorption spectrum of the three sizes of the Ag NWs exhibited two relatively sharp peaks of the SPR position for each diameter. Both absorption bands are liked to longitudinal and transverse plasmon bands. The longitudinal mode stems light extinction processes along the axis of the nanowires, while the transverse mode is driven by analogous mechanisms along the short axis. The results agree with Ref [10].

Upon comparing the three spectra, the longitudinal plasmon band centers of shift from 376.56 nm to 383.3 nm. Meanwhile, the transverse plasmon band centers are located at 350.8 nm, 353.77, and 359.28 nm, respectively. This behavior demonstrates that increasing the diameter of the nanomaterial shifts the absorption spectrum toward longer wavelengths (a redshift) consistent with Ref [18]. As well as, the results also shows that the absorption spectrum of the silver nanomaterial of 50 nm diameter is higher than the absorption spectrum of those of 100 nm and 200 nm in size, due to the high concentration of the Ag NWs when the diameter increases, it obstructs the passage of light, thus reducing the absorption spectrum. This result was supported by [18].

Additionally, the absorbance peak of the Ag nano-hexagonal (Ag NHs) with different sizes (50, 100, and 200 nm) displayed in Figure 3-c, the size of the nanomaterial shows two effects on the position and intensity of the SPR absorption spectrum. The first effect is that increasing the size of the nanomaterial leads to a shift of the absorption spectrum towards long wavelengths (redshift), as it is noticed that the peak is shifted from 413.07 nm to 426.38 nm by increasing the size from 50 nm to 200 nm. While the second effect is that the intensity of the absorption spectrum decreases with increasing the size of the nanomaterial, for the same reason mentioned above.

Details of the absorption peak positions for all samples are presented in Table 1. This difference in values is due to the effect of the size and shape of the nano-silver, as well as to the fact that increasing the refractive index of the medium which leads to modifying the LSPR wavelength of the samples. This result is confirmed by the results presented in Ref [19]. The morphology of the samples is studied to determine the size and shape of the nano-silver and was investigated using FE-SEM, and TEM images, as well as the average size and average diameter calculated by software Image J. The results of the FE-SEM images show that the average size of the Ag NPs changes from 20 nm to 68 nm, when the energy of the laser pulse focused on the silver target changes from 100 mJ to 500 mJ as in the Figure 4. The reason for this is due to the fact that increasing the laser pulse

energy leads to increase in the surface area of the laser beam on target, which results in different penetration depths and different scraping area. This result agrees with [19]. In addition, the TEM results of the Ag nano-hexagonal are displayed in Figure 5.

It can be observed from the TEM images that the hexagonal shape is formed successfully with the different size (50, 100, 200 nm), this is due to the conditions of the chemical reduction experiment and the effect of the auxiliary materials added during the reduction and the testing time changes.

In this scenario, increasing the test time allows the diameter of the Ag NHs to grow, which agrees with [19]. Additionally, the results of the morphological measurements of the Ag NWs are displayed in Figure 6.

The TEM images show that the average diameters of Ag NWs are 50, 100, and 200 nm, with lengths less than 50 microns.

This includes both the TEM images and photographs of the product packaging as received from the German supplier, PlasmaChem Company.

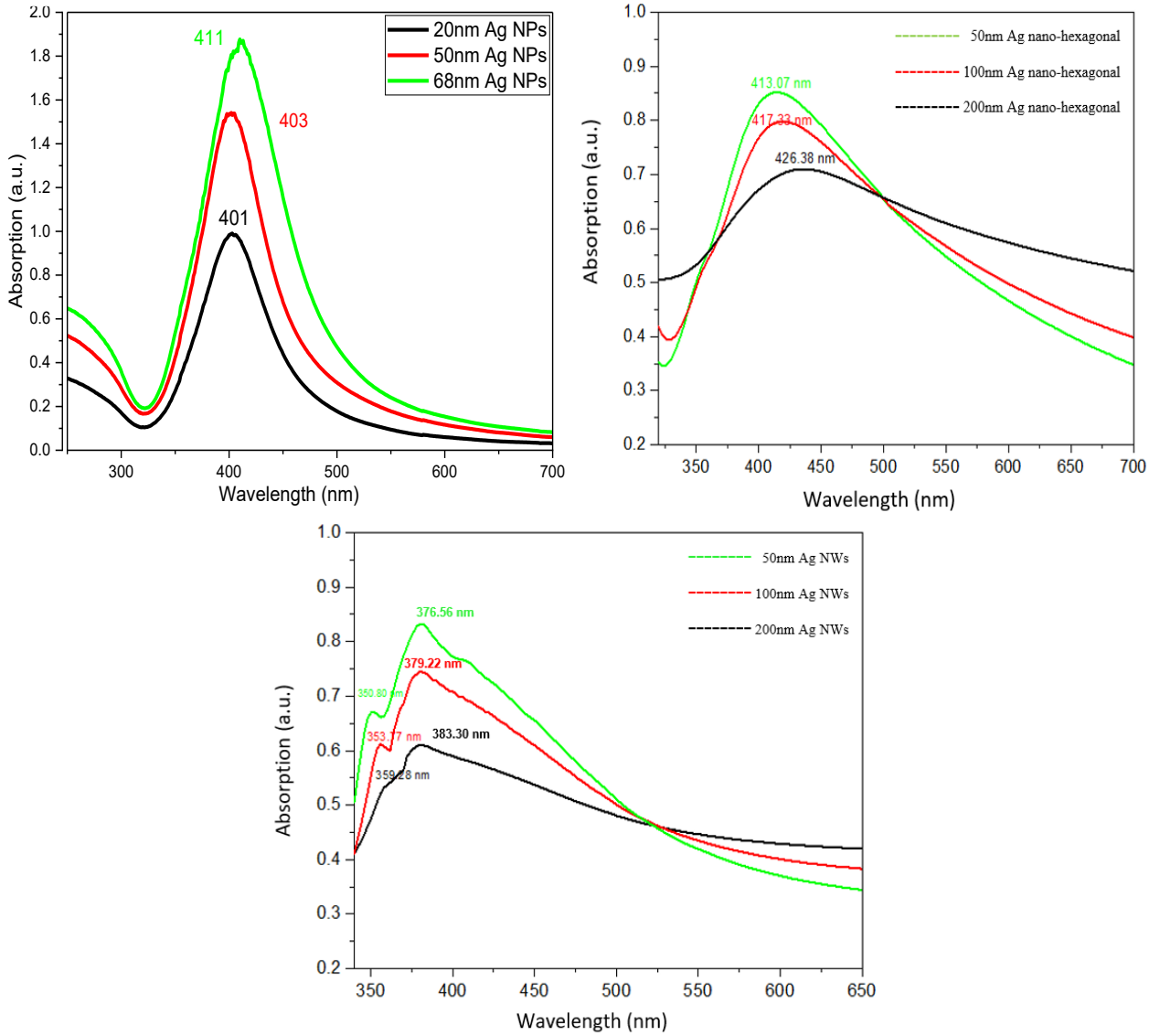

Figure 3. The absorbance spectra of: (a) Ag NPs with different sizes, (b) Ag NHs with different sizes, and (c) Ag NWs with different diameters

Table 1. Absorption peak position controlled by different sizes and shapes of nano-silver

Samples	Shape	Size or Diameter	LSPR position
Ag NPs	spherical	20 nm	401 nm
Ag NPs	spherical	50 nm	403 nm
Ag NPs	spherical	68 nm	411 nm
Ag NHs	hexagonal	50 nm	413.07 nm
Ag NHs	hexagonal	100 nm	417.33 nm
Ag NHs	hexagonal	200 nm	426.38 nm
Ag NWs	wire	50 nm	350.80, 376.56 nm
Ag NWs	wire	100 nm	353.77, 379.22 nm
Ag NWs	wire	200 nm	359.28, 383.30 nm

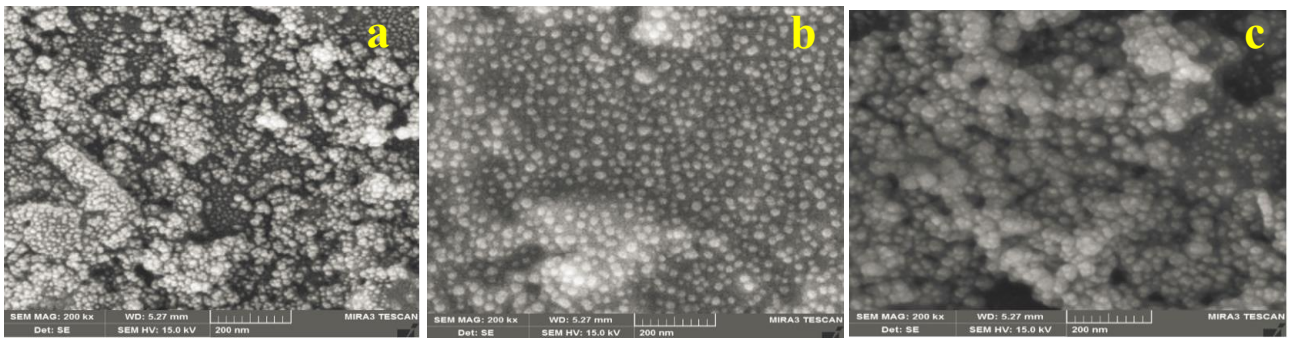

Figure 4. FE-SEM images of the spherical Ag NPs samples: (a) with an average size of 20 nm, (b) with an average size of 50 nm, and (c) with an average size of 68 nm

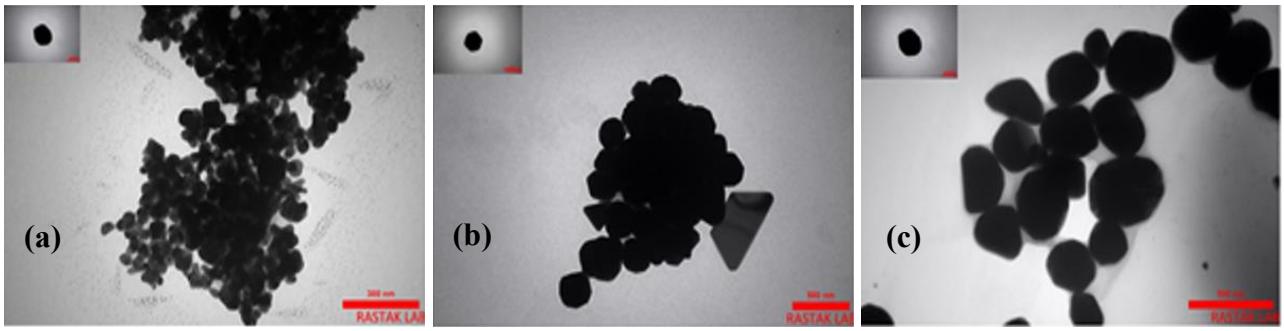

Figure 5. TEM images of the Ag NHs samples: (a) with an average size of 50 nm, b) with an average size of 100 nm, and c) with an average size of 200 nm

Accordingly, the absorption of the nano-silver is exploited in determining temperature rise by applying a suitable illumination compatible with the wavelength of the thermo-plasmonic property. For this purpose, a high-resolution thermal camera (IR camera, model of FLIR) is used to record thermo-plasmonic images of samples. During plasmonic imaging, the samples are irradiated by a continuous laser at a wavelength 405 nm with 50 mW power for 5 min to record the temperature elevation, which is caused by the conversion of light-to-heat with help of the plasmonic nano-silver. The results of the photo-thermal response showed that the nano-silver samples, which are measured by monitoring the temperature change in thermal camera images before and after laser irradiation. In this scenario, thermal response results of the nano-silver samples are displayed in Figure 7. Based on the results, the spherical Ag NPs samples exhibit a higher temperature elevation than the Ag NWs, and the Ag NHs samples.

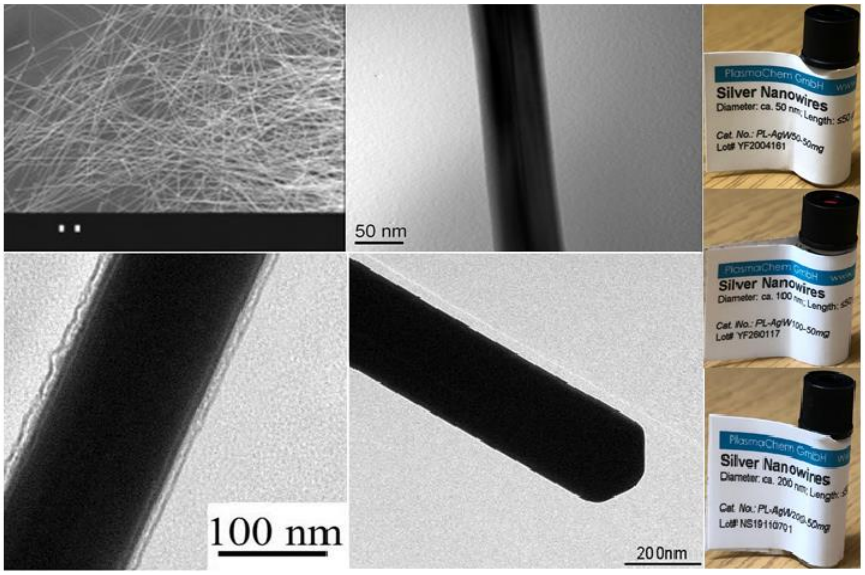

Figure 6. TEM images of the Ag NWs as clusters and of the different diameters in and photographs of the product packaging from the supplier

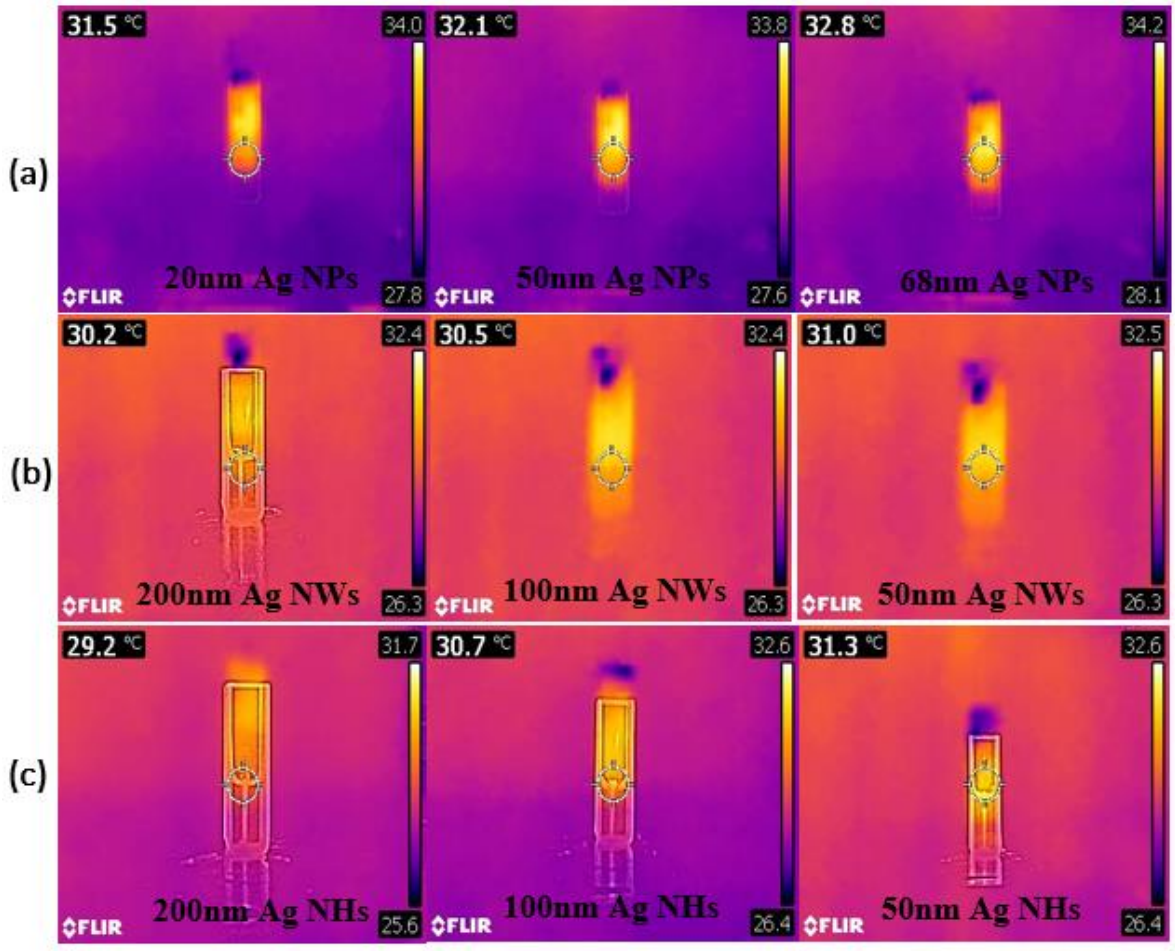

Figure 7. Thermal images recorded by a thermal camera at room temperature for: (a) Ag NPs with different sizes, (b) Ag NWs with different diameters, and (c) Ag NHs with different sizes

While the Ag NHs samples have temperature elevation more than the Ag NWs under laser illumination with fixed conditions.

Therefore, the temperature elevation of the spherical Ag NPs samples increased from 4.5°C to 5.8°C when the size of the Ag NPs increased from 20 nm to 68 nm. While the temperature elevation of the Ag NWs samples increased from 3.2°C to 4.0°C when the diameter of the Ag NWs decreases from 200 nm to 50 nm.

Furthermore, the temperature elevation of the Ag NHs samples increased from 2.2°C to 4.3°C when the size of the Ag NHs decreases from 200 nm to 50 nm. Consequently, the temperature elevation of the nano-silver samples is displayed in Table 2. Results were recorded for all samples under constant conditions (at room temperature 27°C). The results found that the Ag NPs samples have a higher temperature compared to the Ag NWs, and Ag NHs samples, due to the Ag NPs ability to absorb light more than the Ag NWs, and Ag NHs. This result is consistent with the absorption results. The equilibrium temperature is determined by observing the thermometer located in the upper left corner of the thermal image in Figure 7. This is deduced by adding the temperature rise to the room temperature of 27°C. For example, for a 68 nm spherical silver nanoparticle sample, the final temperature reaches approximately 32.8°C (27+5.8°C), which perfectly matches the thermal image in Figure 7. In addition, the samples can reach thermal equilibrium during a 5-minute laser exposure period. During this time, the system reaches a quasi-static equilibrium where the energy absorbed from the laser is balanced by the energy dissipated or lost to the surroundings. Our results show that the efficiency of this equilibrium varies depending on the size and geometry of the silver nanoparticles. Spherical shapes of silver nanoparticles tend to retain heat better, while shapes with extensions or geometric surfaces, such as nanowires and hexagonal structures, dissipate heat more quickly to the surrounding environment. It is known that the thermal time constant depends primarily on two factors: the heat capacity of the system and the thermal resistance of conduction or dissipation. In this experiment, the time constant of the silver nanoparticles is very short compared to the total irradiation period, with the system reaching thermal stability within a few minutes of laser exposure. This is determined by observing the temperature change over the experiment and depends on the shape and size of the silver nanoparticles. Remarkably, one of the important results that can be observed is that the spherical metal nano-system retains the absorbed heat inside it, which makes it heat up more. While the geometric metal nano-system that contains edges or extensions such as hexagonal or cylindrical dissipates the absorbed heat to the surroundings more than the spherical nano-system. Moreover, the results showed that the temperature increase of the nano-system proposed in this study, it encourages many applications including disinfection and sterilization of medical surgical equipment. In the next step, the nonlinear optical properties results measured by the z-scan technique, which included measuring a nonlinear refractive index of nano-silver samples. The results showed that the Ag NPs samples have the nonlinear refractive index value greater than that of the Ag NHs and the Ag NWs samples. The results that the nonlinear refractive index values of the Ag NHs are higher than those of the Ag NWs. This means that the nonlinear refractive index of spherical or semi-spherical suspensions is larger than other shapes under the same laser conditions used for measurement. The results indicate the fact that the nonlinear refractive index of nano-silver increases with increasing particle size when the shape of the nano-silver is constant, as well as the peak-valley in the z-scan spectrum has been observed indicating that the nonlinear refractive index exhibits a negative sign for all nano-silver samples.

Table 2. Temperature elevation for all samples under illumination with a 50 mW laser at 405 nm for 5 min.

Samples	Shape	Size or Diameter	Temperature Elevation ΔT (°C)	Heating Rate = ΔT °C / 5 min
Ag NPs	spherical	20 nm	4.5	0.9
Ag NPs	spherical	50 nm	5.1	1.02
Ag NPs	spherical	68 nm	5.8	1.16
Ag NWs	wire	50 nm	4.0	0.8
Ag NWs	wire	100 nm	3.5	0.7
Ag NWs	wire	200 nm	3.2	0.64
Ag NHs	hexagonal	50 nm	4.3	0.86
Ag NHs	hexagonal	100 nm	3.7	0.74
Ag NHs	hexagonal	200 nm	2.2	0.44

The effects of the size and shape of the nano-silver on the nonlinear refractive index were studied. We observed an increase in the size and diameter of the nano- silver leads to increasing the distance between the peak-valley transmittance as shown in Figure 8, thus increasing the nonlinear refractive index of all samples, as shown in Table 3. The reason for this is that various physical mechanisms directly affecting the nonlinear refractive index include, these effects include electrostriction, photorefractive, electronic polarization, ultrafast electronic, and thermal effect [20]. In our case, thermal effects are the most influential. Thus, this effect increases with increasing size of the nano-silver, as the results of the thermo-plasmonic confirm this.

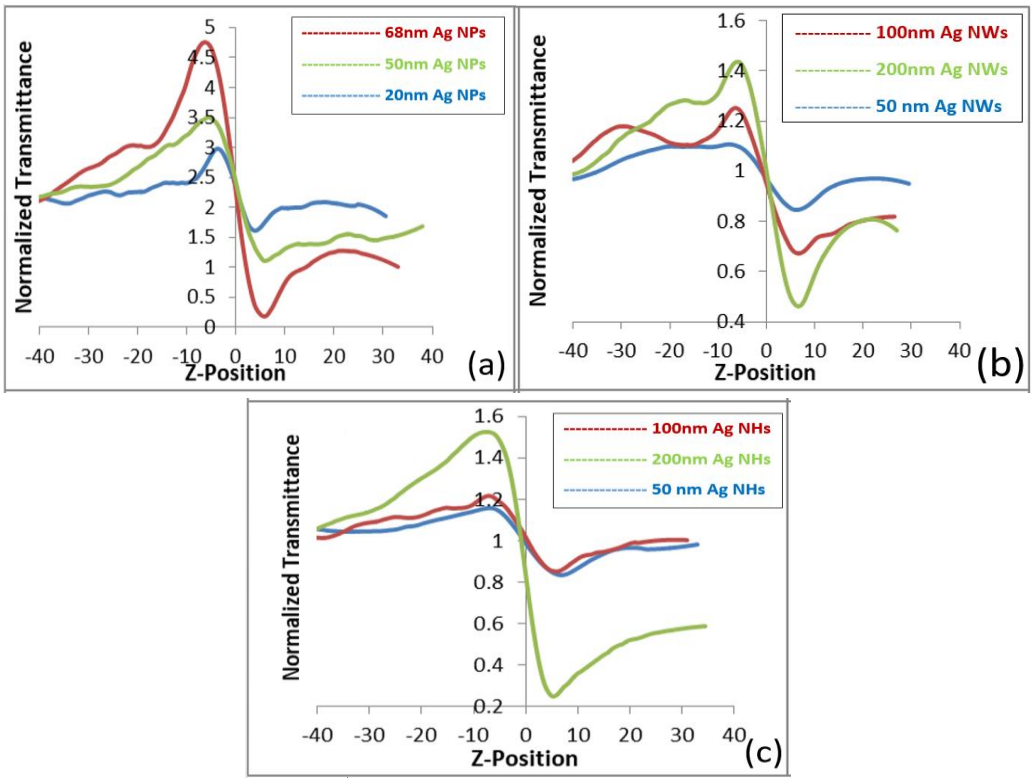

Figure 8. Z-scan spectrum of the nano-silver: (a) Ag NPs with different sizes, (b) Ag NWs with different diameters, and (c) Ag NHs with different sizes

Table 3. Nonlinear refractive index of the nano-silver for all samples

Samples	Shape	size or Diameter	Nonlinear refractive index (cm^2/watt)
Ag NPs	spherical	20 nm	- 1.253 E-12
Ag NPs	spherical	50 nm	- 1.627 E-12
Ag NPs	spherical	68 nm	- 2.332 E-12
Ag NWs	wire	50 nm	- 0.335 E-12
Ag NWs	wire	100 nm	- 0.561 E-12
Ag NWs	wire	200 nm	- 0.954 E-12
Ag NHs	Hexagonal	50 nm	- 0.366 E-12
Ag NHs	Hexagonal	100 nm	- 0.642 E-12
Ag NHs	Hexagonal	200 nm	- 1.189 E-12

4. Conclusions

We conclude from the current study that the pulsed laser ablation in liquid method, and the chemical method are methods that are successfully used to generate the nano-silver with tunable and controllable properties. Thus, changing the size of the Ag NPs by changing the laser energy used for ablation, and changing the diameter of the Ag NWs by changing the time of the chemical experiment, with the possibility of controlling the plasmonic properties to achieve the desired photo-thermal response of the nano-silver.

The results show that the Ag NPs are more capable of generating the thermo-plasmonic effects compared to the Ag NWs under the same conditions. Instead, thermal properties can also be improved by increasing the diameter and size of the nano-silver which leads to efficient enhancement in the photo-thermal response of samples. Thus obtaining improved nonlinear optical properties. Results have also proven that the proposed nano-system demonstrated usefulness in multiple applications including biomedical applications.

Conflict of Interest: The authors of this manuscript affirm that there is no conflict of interest regarding the publication of this work.

Funding: This work was supported by the Department of Laser Physics, College of Science for Women, University of Babylon, Hilla, Iraq.

Author contributions: Nada A. Mohammed: Experimental work and writing. Hassan A. Majeed: Initial experimental work. Ahmed. K. Kodeary: Conceptualization, Supervision, Validation, Writing Review & Editing.

References

[1] Mbarak, H., A.K. Kodeary, S.M. Hamidi, E. Mohajarani, and Y. Zaatar. "Control of nonlinear refractive index of AuNPs doped with nematic liquid crystal under external electric field." *Optik* 198 (2019), 163299. https://doi.org/10.1016/j.ijleo.2019.163299

[2] Pathak, Nilesh K., Partha Sarathi, and Gyanendra K. Pandey. "Comparative study of thermoplasmonic effects of gold and silver metal nanoparticle." *AIP Advances* 11, no. 4 (2021). https://doi.org/10.1063/5.0046284

[3] Biranvand, Neda, Ali Bahari, Hanieh Yazdanfar, Ahmed K. Kodeary, and Seyedeh M. Hamidi. "Nonlinear refractive index of the gold nanoparticle/silicon quantum dot hybrid structure." *Physica Scripta* 97, no. 3 (2022), 030001.

https://doi.org/10.1088/1402-4896/ac52fb

[4] Qayyum, Hamza, Samar Mamdouh, Alaa Mahmoud, and Tarek Mohamed. "Nonlinear Optical Properties of Silver Nanoparticles: A Comprehensive Review." *Laser Innovations for Research and Applications* 2, no. 2 (2025), 0-0. https://doi.org/10.21608/lira.2025.383757.1007

[5] Gatea, Maher A., Hussein A. Jawad, and S. M. Hamidi. "Detecting the thermoplasmonic effect using ellipsometry parameters for self-assembled gold nanoparticles within a polydimethylsiloxane matrix." *Applied Physics A* 125, no. 2 (2019). https://doi.org/10.1007/s00339-019-2401-7

[6] Karwi, Zahraa L., Ahmed K. Kodeary, and Ferydon Babaei. "Antifungal Activity Based on Enhancement of Thermoplasmonic Properties of Hybrid Nanostructures Prepared by Laser Ablation in Liquid." *Plasmonics*, 2024. https://doi.org/10.1007/s11468-024-02392-4

[7] Chen, Yong, and Hai Ming. "Review of surface plasmon resonance and localized surface plasmon resonance sensor." *Photonic Sensors* 2, no. 1 (2012), 37-49. https://doi.org/10.1007/s13320-011-0051-2

[8] Taheri, Majid, S. Parhizkar, and H. Farrokhi. "Shape dependent nonlinear optical response of silver nanocrystals." *Journal of Russian Laser Research* 46, no. 4-6 (2025), 143-155. https://doi.org/10.1007/s10946-025-10265-2

[9] Mashayekh, Maryam, and Davoud Dorranian. "Size-dependent nonlinear optical properties and thermal lens in silver nanoparticles." *Optik* 125, no. 19 (2014), 5612-5617. https://doi.org/10.1016/j.ijleo.2014.07.066

[10] Fadel, Adwa H., Hamsa N. Naser, and Ahmed K. Kodeary. "Tunable photo-thermal response and plasmonic properties based on the different size and shape of nano-gold." *AIP Conference Proceedings* 3405 (2026), 050007. https://doi.org/10.1063/5.0318449

[11] Panda, S. K., S. Chakraborti, and R. N. Basu. "Size and shape dependences of the colloidal silver nanoparticles on the light sources in photo-mediated citrate reduction technique." *Bulletin of Materials Science* 41, no. 4 (2018). https://doi.org/10.1007/s12034-018-1609-z

[12] Yeshchenko, Oleg A., Igor M. Dmitruk, Alexandr A. Alexeenko, Andriy V. Kotko, James Verdal, and Anatoliy O. Pinchuk. "Size and Temperature Effects on the Surface Plasmon Resonance in Silver Nanoparticles." *Plasmonics* 7, no. 4 (2012), 685-694. https://doi.org/10.1007/s11468-012-9359-z

[13] Un, Leng-Wai, and Yonatan Sivan. "Thermo-optical nonlinearity of metallic nanoparticle(s)." *Photonic and Phononic Properties of Engineered Nanostructures XI*, 2021, 17. https://doi.org/10.1117/12.2582737

[14] Karwi, Zahraa L., Ahmed K. Kodeary, and Ferydon Babaei. "Investigated numerically nanoshell thickness on photothermal response of hybrid nanostructures in an aqueous medium." *Optik* 313 (2024), 172007. https://doi.org/10.1016/j.ijleo.2024.172007

[15] Pathak, Nilesh K., Partha Sarathi, and Gyanendra K. Pandey. "Comparative study of thermoplasmonic effects of gold and silver metal nanoparticle." *AIP Advances* 11, no. 4 (2021). https://doi.org/10.1063/5.0046284

[16] Ejbarah, R., A. Kodeary, Talib Abbas, and Seyedeh M. Hamidi. "Magneto - Plasmonic Properties of Hybrid Nanostructures Prepared by Laser Ablation in Different Solutions." 2023. https://doi.org/10.2139/ssrn.4392379

[17] Kodeary, A. K., M. A. Gatea, S. F. Haddawi, and S. M. Hamidi. "Tunable thermo-piezo-plasmonic effect on core/shell nanoparticles under laser irradiation and external electric field." *Optical and Quantum Electronics* 52, no. 2 (2020). https://doi.org/10.1007/s11082-020-2232-y

[18] Kodeary, A.K., S.M. Hamidi, and R. Moradlou. "Voltage controlled properties of piezo-magneto-plasmonic core/shell nanoparticles." *Nano-Structures & Nano-Objects* 21 (2020), 100415. https://doi.org/10.1016/j.nanoso.2019.100415

[19] Amendola, Vincenzo, and Moreno Meneghetti. "Laser ablation synthesis in solution and size manipulation of noble metal nanoparticles." *Physical Chemistry Chemical Physics* 11, no. 20 (2009), 3805. https://doi.org/10.1039/b900654k

[20] Liu, Guohua. "Fundamental Principles of Thermoplasmonics." *Thermoplasmonics*, 2024, 7-39. https://doi.org/10.1007/978-981-97-8332-8_2